Journal of Cellular and Molecular Medicine
A JOURNAL OF TRANSLATIONAL MEDICINE

J. Cell. Mol. Med. Vol 15, No 12, 2011 pp. 2684-2696

Cyclic ADP ribose is a novel regulator of intracellular Ca^{2+} oscillations in human bone marrow mesenchymal stem cells

Rong Tao [a], Hai-Ying Sun [a], Chu-Pak Lau [a], Hung-Fat Tse [a], Hon-Cheung Lee [b], Gui-Rong Li [a, b, *]

[a] *Department of Medicine, Li Ka Shing Faculty of Medicine, The University of Hong Kong, Pokfulam, Hong Kong SAR, China*
[b] *Department of Physiology, Li Ka Shing Faculty of Medicine, The University of Hong Kong, Pokfulam, Hong Kong SAR, China*

Received: September 7, 2010; Accepted: January 6, 2011

Abstract

Bone marrow mesenchymal stem cells (MSCs) are a promising cell source for regenerative medicine. However, the cellular biology of these cells is not fully understood. The present study characterizes the cyclic ADP-ribose (cADPR)-mediated Ca^{2+} signals in human MSCs and finds that externally applied cADPR can increase the frequency of spontaneous intracellular Ca^{2+} ($Ca^{2+}{}_i$) oscillations. The increase was abrogated by a specific cADPR antagonist or an inositol trisphosphate receptor (IP3R) inhibitor, but not by ryanodine. In addition, the cADPR-induced increase of $Ca^{2+}{}_i$ oscillation frequency was prevented by inhibitors of nucleoside transporter or by inhibitors of the transient receptor potential cation melastatin-2 (TRPM2) channel. RT-PCR revealed mRNAs for the nucleoside transporters, concentrative nucleoside transporters 1/2 and equilibrative nucleoside transporters 1/3, IP3R1/2/3 and the TRPM2 channel, but not those for ryanodine receptors and CD38 in human MSCs. Knockdown of the TRPM2 channel by specific short interference RNA abolished the effect of cADPR on the $Ca^{2+}{}_i$ oscillation frequency, and prevented the stimulation of proliferation by cADPR. Moreover, cADPR remarkably increased phosphorylated extracellular-signal-regulated kinases 1/2 (ERK1/2), but not Akt or p38 mitogen-activated protein kinase (MAPK). However, cADPR had no effect on adipogenesis or osteogenesis in human MSCs. Our results indicate that cADPR is a novel regulator of $Ca^{2+}{}_i$ oscillations in human MSCs. It permeates the cell membrane through the nucleoside transporters and increases Ca^{2+} oscillation *via* activation of the TRPM2 channel, resulting in enhanced phosphorylation of ERK1/2 and, thereby, stimulation of human MSC proliferation. This study delineates an alternate signalling pathway of cADPR that is distinct from its well-established role of serving as a Ca^{2+} messenger for mobilizing the internal Ca^{2+} stores. Whether cADPR can be used clinically for stimulating marrow function in patients with marrow disorders remains to be further studied.

Keywords: human bone marrow • mesenchymal stem cells • cyclic ADP ribose • TRPM2 • calcium signalling

Introduction

It is well recognized that bone marrow-derived mesenchymal stem cells (MSCs) are present within the bone marrow cavity and serve as a reservoir for the continuous renewal of various mesenchymal tissues [1–4]. MSCs have recently been moved into the main stream focus by virtue of their plasticity and potential applications in various clinical situations [2, 5], such as tissue regeneration and haematopoietic stem cell transplantation [1, 6]. In addition, MSCs were widely used for the studies of adipogenic and osteogenic differentiation [1–4]. However, their cellular biology is not fully understood, especially on the regulation of their cellular activities by the cytosolic free calcium ion ($Ca^{2+}{}_i$).

$Ca^{2+}{}_i$ functions as a highly versatile secondary messenger in virtually all types of eukaryotic cells and regulates a wide range of cellular functions, including the regulation of ion channel, gene transcription, cell proliferation and differentiation [7]. It is generally recognized $Ca^{2+}{}_i$ are usually mediated by inositol trisphosphate receptors (IP3Rs) and ryanodine receptors (RyRs). Kawano and colleagues were the first to demonstrate that human MSCs exhibit spontaneous $Ca^{2+}{}_i$ oscillations that are initiated by autocrine/paracrine ATP *via* the activation of the IP3R-mediated Ca^{2+} release, but not RyRs, because no RyRs are detected in these cells [8–10]. The physiological role of the Ca^{2+} oscillation is unknown but may be important in regulating cellular proliferation. Indeed, it has been reported in other cells that the frequency of

*Correspondence to: Dr. Gui-Rong LI,
L4–59, Laboratory Block, FMB, The University of Hong Kong,
21 Sassoon Road, Pokfulam,
Hong Kong SAR, China.
Tel.: 852–2819-9513
Fax: 852–2855-9730
E-mail: grli@hkucc.hku.hk

doi: 10.1111/j.1582-4934.2011.01263.x

$Ca^{2+}{}_i$ sparks determines the gene expression efficiency [11] and controls kinase activities [12]. Consistently, a recent study demonstrated that the flow stress-manipulated $Ca^{2+}{}_i$ oscillations in human MSCs can indeed regulate proliferation [13].

Cyclic adenosine diphosphate ribose (cADPR) has been recognized as a universal Ca^{2+} mobilizer by activating RyRs in many types of cells [14–16]. In addition, cADPR has been reported to mediate Ca^{2+} entry by activating transient receptor potential cation channel melastatin-2 (TRPM2) [14, 17, 18]. It plays an important role in the regulation of various cellular behaviours, including insulin secretion [19] and cell proliferation [20]. cADPR has been attributed as a non-peptide haematopoietic growth factor because of its unique role in the stimulation of proliferation of human MSCs [21] and its regulation of human haematopoiesis [22–24]. However, the specific mechanism involved is unknown. The present study was thus designed to investigate the mechanism of cADPR in regulating Ca^{2+} signalling in human MSCs during proliferation as well as during adipogenic and osteogenic differentiation. The results from this study demonstrate an alternate signalling pathway of cADPR that is distinct from its well-established role of serving as a Ca^{2+} messenger for mobilizing the internal Ca^{2+} stores in human MSCs, which provide important information that human bone marrow function may be regulated by Ca^{2+} signalling.

Materials and methods

Human MSCs culture

Human bone marrow MSCs at passage 1 were generously provided by Dr. Darwin J. Prockop, Texas A&M Health Science Center College of Medicine Institute for Regenerative Medicine at Scott & White. The cells were characterized of positive for surface markers CD44, CD90, CD166, CD105, CD29, CD49c, CD147, CD59 and human leukocyte antigen-1 (HLA-1), and negative for CD34, CD36, CD45, CD184 and CD106 (Table S5). These cells have been tested for successful bone and fat differentiation. The cells were cultured at 37°C in 95% air and 5% CO_2, in the growth medium, *i.e.* minimal essential medium α (α-MEM, Invitrogen, Hong Kong, China) contained 15% foetus bovine serum (FBS; Hyclone, Logan, UT, USA), 2 mM glutamine, 100 U/ml penicillin and 100 μg/ml streptomycin. When cells grew to 70–80% confluence, they were lifted by 0.25% trypsin and 1 mM ethylenediaminetetraacetic acid (EDTA) in phosphate-buffered saline (PBS) solution for subculture as described previously [25].

Differentiation induction

Adipogenesis.

Human MSCs were plated into 6-well plates in growth medium and the growth medium was changed to adipogenic medium (α-MEM supplemented with 10% FBS, 1 μM dexamethasone, 0.5 mM 3-isobutyl-1-methylxanthine, 50 μM indomethacin and 10 μg/ml insulin) when cells reached confluence. After 3 days induction, the adipogenic medium was replaced by maintenance medium (α-MEM supplemented with 10% FBS and 10 μg/ml insulin) and maintained for 2 days. After one, two or three cycles of induction and maintenance, plates were fixed with 4% PBS buffered paraformaldehyde solution at 4°C for 1 hr. Followed with washes with PBS to remove paraformaldehyde, Oil red O staining solution was added to visualize the oil drops in differentiated cells.

Osteogenesis.

Human MSCs were plated into 6-well plates in growth medium. When cells grew to confluence, the growth medium was changed to osteogenic medium (α-MEM supplemented with 10% FBS, 100 nM dexamethasone, 10 mM β-glycerol phosphate and 50 μM L-ascorbic acid-2-phosphate). The osteogenic medium was replaced every 3 days. After 10, 15 or 20 days induction, plates were processed to fixation with PBS buffered 4% paraformaldehyde and staining with Alizarin red S for visualization of mineralization [26].

Reverse transcription and polymerase chain reaction

The reverse transcription and polymerase chain reaction (RT-PCR) was performed as previously described [25, 27, 28]. Briefly, total RNA extraction was performed with Trizol extraction system. RNA pellet was obtained by centrifuge and total RNA was treated with DNase I (GE Healthcare, Hong Kong, China) to remove genomic DNA at 37°C for 30 min. RT was performed with the Promega Reverse Transcription System (Promega, Madison, WI, USA) in a 20-μ1 reaction mixture. The cDNA product from RT reaction was used for PCR amplification of specific gene expression.

PCR primers were designed with human genes using Primer Premier 5 software (Premier Biosoft international, Palo Alto, CA, USA) and synthesized at the Genome Research Center at the University of Hong Kong. The forward and reverse PCR oligonucleotide primers chosen to amplify the cDNA are listed in (Tables S1–S3). PCR was performed with a Promega PCR system with Taq polymerase and accompanying buffers. The thermal cycling conditions were: 94°C for 2 min., 28–30 cycles of 94°C (45 sec.), 58°C (45 sec.) and 72°C (1 min.). This was followed by a final extension at 72°C (10 min.) to ensure complete product extension. The PCR products were then electrophoresed through a 1.5% agarose gel, and the amplified cDNA bands were visualized using ethidium bromide staining and imaged using Chemi-Genius Bio Imaging System (Syngene, Cambridge, UK).

Western blot

Western blot was performed as previously described [27]. Briefly, Cells at 70~80% confluence were lysed with a modified RIPA buffer containing (in mM) 50 Tris-HCl, 150 NaCl, 1 EDTA, 1 phenylmethylsulfonyl fluoride, 1 sodium orthovanadate, 1 NaF, 1 μg/ml aprotinin, 1 μg/ml leupeptin, 1 μg/ml pepstatin, 1% NP-40, 0.25% sodium deoxycholate, 0.1% SDS. Protein concentration was determined by Bio-Rad (Bio-Rad Laboratories, Hercules, CA, USA) protein assay. Cell lysates (50 μg) were mixed with sample buffer and denaturated by heating to 95°C for 5 min. Samples were resolved *via* SDS-PAGE and transferred to nitrocellulose membranes. Membranes were blocked with 5% non-fat milk in Tris Buffer Saline with Tween-20 (TTBS) then probed with primary antibodies (1:500–1000) at 4°C overnight with agitation. Anti-Akt, anti-p-Akt, anti-ERK1/2 (extracellular-signal-regulated kinases 1/2), anti-p-ERK1/2, anti-p38 and anti-p-p38

antibodies were from Millipore (Billerica, MA, USA), while anti-TRPM2 and anti-c-Jun N-terminal kinase (JNK), anti-PPAR-γ (peroxisome proliferator-activated receptor γ), and anti-osteocalcin antibodies were from Santa Cruz Biotech (Santa Cruz, CA, USA). After washing with TTBS, the membranes were incubated with HRP-conjugated goat anti-rabbit or donkey anti-goat IgG antibody (Santa Cruz Biotech) at 1:4000 dilutions in TTBS at room temperature for 1 hr. Membranes were washed again with TTBS then processed to develop x-ray film using an enhanced chemiluminescence detection system. The relative band intensities were measured by quantitative scanning densitometer and image analysis software (Bio-1D, version 97.04, Froebel, Wasserburg, Germany).

$Ca^{2+}{}_i$ measurements

$Ca^{2+}{}_i$ activity was measured using confocal microscopy scanning technique as described previously [29, 30] in human MSCs. The cells were loaded with 5 μM fluo-3 acetoxymethyl ester (AM) (Biotium, Hayward, CA, USA) in the culture medium for 30 min. at 37°C, and then rinsed with PBS to remove extracellular fluo-3 AM and incubated in Tyrode solution at room temperature for 30 min. before recording $Ca^{2+}{}_i$ signals. Tyrode solution contained (in mM): 140 NaCl, 5.4 KCl, 1 $MgCl_2$, 1.8 $CaCl_2$, 0.33 NaH_2PO_4, 10 4-(2-hydroxyethyl)-1-piperazineethanesulfonic acid (HEPES) and 10 glucose (pH = 7.3). $Ca^{2+}{}_i$ was monitored every 10 sec. in human MSCs using a confocal microscopy (Olympus FV300, Tokyo, Japan) at room temperature (22–23°C). Fluo-3 was excited at 488 nm and emission was detected at >505 nm.

RNA interference

Short interference RNA (siRNA) molecules targeting different exons of TRPM2 gene were synthesized by Ambion Company (Austin, TX, USA). Specific sequences for target genes are shown in Table S4. A FAM-labelled sequence which has no known target in the human genome was used as a negative control (*i.e.* control siRNA). The siRNA segments (final concentrations at 50 nM as recommended by the supplier) were transfected into human MSCs at 50–60% confluence using lipofectamine 2000 (Invitrogen) as described previously [27] or in supplemental experimental procedures.

Cell proliferation assays

MTT (3-(4,5-dimethyl-thiazol-2-yl)-2,5-diphenyl tetrazolium bromide) assay was applied to assess the effects of ion channel blockers on cell proliferation [27]. Human MSCs were plated into 96-well plate at a density of 5×10^4 cells per well in 200 μl complete culture medium. After 8 hrs recovery, the culture medium containing ion channel blockers was employed. Following 72 hrs cADP ribose incubation, 20 μl PBS buffered MTT (5 mg/ml) solution was added to each well and the plates were incubated at 37°C for additional 4 hrs. The medium was removed and 100 μl/well dimethyl sulfoxide was added to each well to dissolve the purple formazan crystals. The plates were read (wavelengths: test, 570; reference, 630 nm) using a μQuant microplate spectrophotometer (Bio-Tek Instruments, Inc., Winooski, VT, USA). Results were standardized using control group values.

[^{3}H]-thymidine incorporation assay was introduced to assess proliferating cell rate [27]. Human MSCs were plated into 96-well plate at a density of 5×10^4 cells per well in 200 μl complete culture medium. After 8 hrs recovery, the culture medium was replaced with a medium containing cADP ribose or TRPM2 siRNAs and incubated for 48 hrs, then 1 μCi (0.037 MBq) ^{3}H-thymidine (GE Healthcare) was added into each well. Following additional 24 hrs incubation, cells were harvested and transferred to a nitrocellulose coated 96-well plate *via* suction. Nitrocellulose membrane was washed with water flow and plate was air dried at 50°C overnight. Liquid scintilla (20 μL per well) was then added to each well. Counts per minute for each well were read by a TopCount microplate scintillation and luminescence counter (PerkinElmer, Waltharn, MA, USA).

Statistical analysis

Results are presented as means ± S.E.M. Paired and/or unpaired Student's t-tests were used as appropriate to evaluate the statistical significance of differences between two group means, and ANOVA was used for multiple groups. Values of $P < 0.05$ were considered to indicate statistical significance.

Results

Characterization of the human MSCs

Human MSCs (passage 4) showed a fibroblast-like appearance at day 3 after sub-culturing and became confluence at day 8 (Fig. 1). Figure 1B and C display adipogenic and osteogenic differentiation in human MSCs at passage 5. The cells could be induced to differentiate efficiently into adipocytes (Fig. 1B) or osteocytes (Fig. 1C), which occurred, however, only after specific induction. RT-PCR (Fig. 1D) revealed the expression of lineage-specific genes after induction: PPAR-γ and fatty acid binding protein 4 for adipocytes, and runt related transcription factor 2 and osteocalcin for osteocytes [2, 31]. The PCR primers used for detection of these specific genes are shown in Table S1. These results indicate that human MSCs we studied here are maintained in the 'stem' state before induction.

We found that the amplitude (1–3 arbitrary units) and frequency (oscillation/2.5–13 min.) of the spontaneous $Ca^{2+}{}_i$ oscillations were variable from cell to cell (Fig. 1E and F). The percentage of human MSCs exhibiting spontaneous $Ca^{2+}{}_i$ oscillations varied between 86% (110 of 128 cells) in passage 2 cells and 78% (100 of 128 cells) in passage 5 cells (Fig. 1G). The percentage was further reduced to only 12.5% at passage 10 (6 of 128 cells, data not shown), which is most likely related to cell senescence in culture [32–34]. Therefore, only human MSCs at passages 2–5 were used in all subsequent experiments.

Spontaneous $Ca^{2+}{}_i$ oscillations in human MSCs were not related to RyRs [8]. Here, we further confirmed that the spontaneous $Ca^{2+}{}_i$ oscillations in human MSCs were inhibited by the IP3 inhibitor, 2-aminoethoxydiphenyl borate, the sarco/endoplasmic reticulum Ca^{2+}-ATPase (SERCA) inhibitor, cyclopiazonic acid and the SOC channel inhibitor, La^{3+}, but not by ryanodine (Fig. S1A–D). Moreover, RT-PCR also revealed the expression of three types of IP3Rs (1/2/3), SERCAs (1/2/3), plasma membrane Ca^{2+} ATPase (PMCAs) (1/2/3) and Na^+-Ca^{2+} exchanger (NCX) (1/3/4) in human MSCs, but not RyRs (Fig. S1E, F).

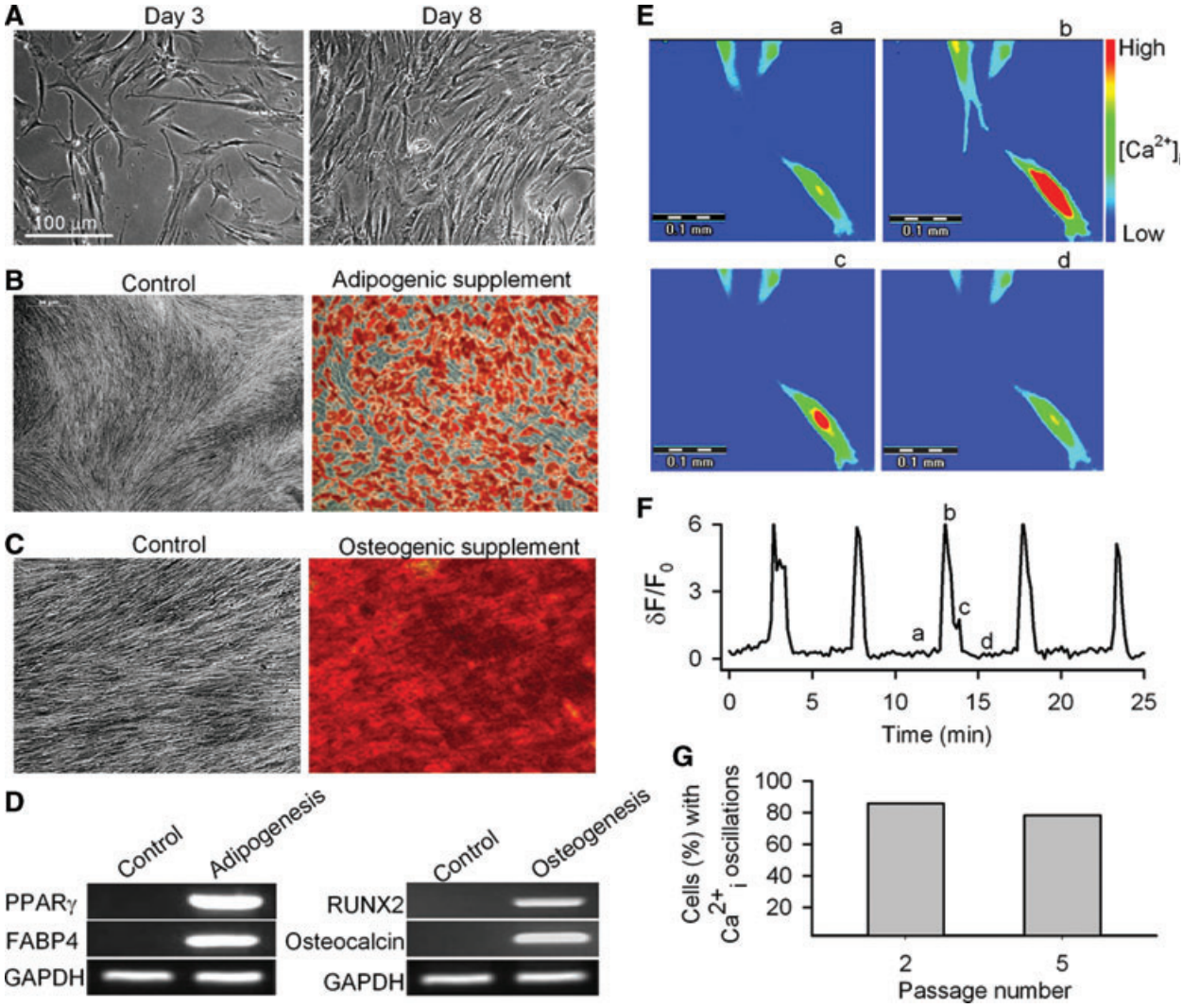

Fig. 1 Characteristics of human MSCs. (**A**) Cells in culture on day 3 (left) and day 8 (right) from subculture from passage 4. (**B**) Adipogenic differentiation of human MSCs (passage 5) in control (left) and adipogenic supplement (right). Cells were stained with Oil red O. (**C**) Osteogenic differentiation of human MSCs (passage 5) in control (left) and osteogenic supplement (right). Cells were stained with Alizarin red S. (**D**) RT-PCR revealed the lineage-specific genes expression in cells from controls and adipogenic and osteogenic differentiation cultures. PPAR-γ: peroxisome proliferator-activated receptor gamma; FABP4: fatty acid binding protein 4; RUNX2: runt related transcription factor 2. (**E**) 'Pseudo'-colour images show changes in fluorescence intensity (*i.e.* $Ca^{2+}{}_i$) in the cell at time-points a, b, c, d, as indicated in (**F**). (**F**) Spontaneous $Ca^{2+}{}_i$ oscillations observed in a representative cell from passage 3. The pseudo-ratio $\delta F/F_0$: $\delta F/F_0 = (F - F_{base})/F_{base}$ was applied to express $Ca^{2+}{}_i$ level, where F is the measured fluorescence intensity of Fluo-3, F_{base} is the lowest level of fluorescence intensity in the cell. (**G**) Incidence of spontaneous $Ca^{2+}{}_i$ oscillations in human MSCs from passages 2 and 5.

Cyclic ADP ribose and $Ca^{2+}{}_i$ oscillations in human MSCs

Figure 2A shows that the addition of cADPR (50 μM) to the bath solution did not induce Ca^{2+} changes in the cells exhibiting no spontaneous $Ca^{2+}{}_i$ oscillations ($n = 16$). However, cADPR (10 and 50 μM) remarkably enhanced the $Ca^{2+}{}_i$ oscillation frequency in cells with spontaneous $Ca^{2+}{}_i$ oscillations (Fig. 2B and C). 8-Br-cADPR (100 μM), a specific antagonist of cADPR, had no effect on the spontaneous $Ca^{2+}{}_i$ oscillations, but prevented the enhancing effect of cADPR on the oscillation frequency (Fig. 2D). Interestingly, the enhancement of the $Ca^{2+}{}_i$ oscillation frequency by cADPR was not affected by 30 μM ryanodine (Fig. 2E). The IP3Rs blocker [8] 2-aminoethoxydiphenyl borate (50 μM), which is also a blocker of TRPM2 channels [35],

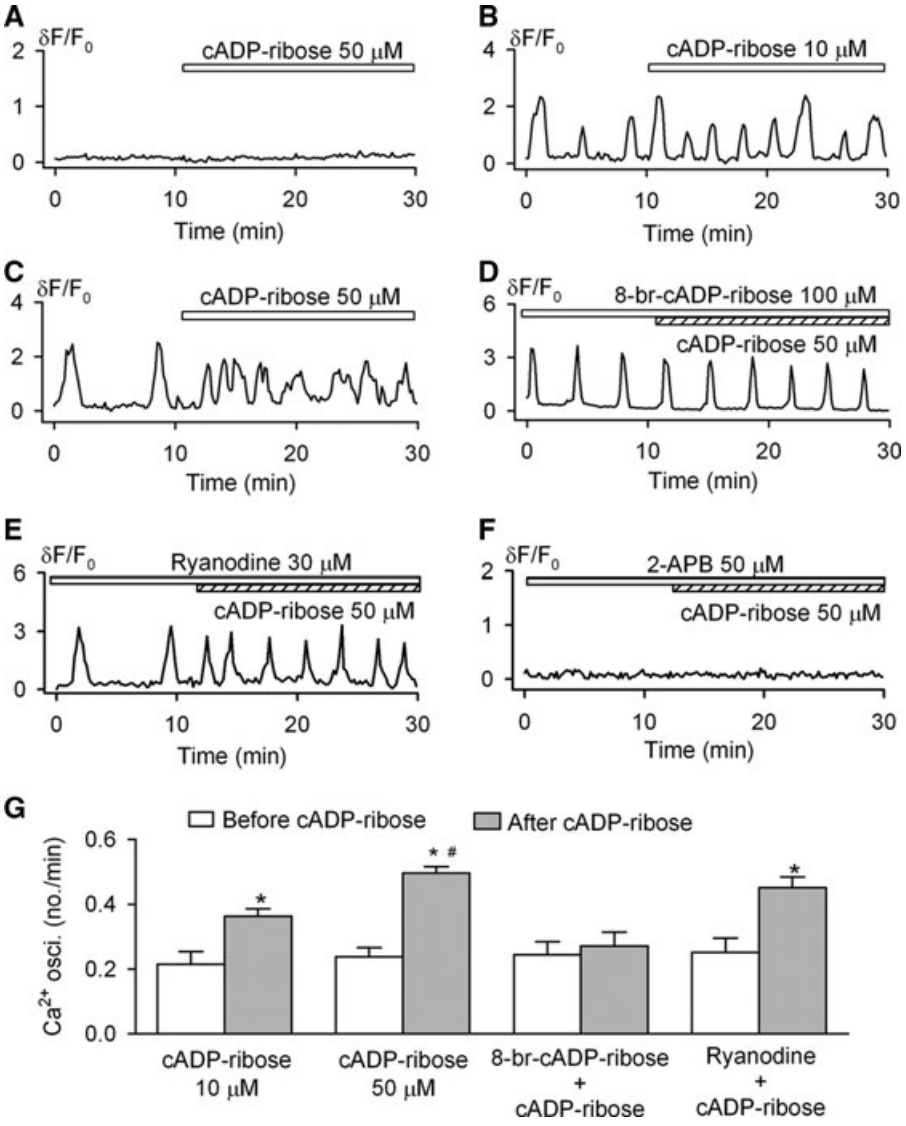

Fig. 2 Effects of cADPR on spontaneous $Ca^{2+}{}_i$ oscillations. (**A**) Cyclic ADP ribose did not initiate $Ca^{2+}{}_i$ transient or $Ca^{2+}{}_i$ oscillations in the cell without spontaneous $Ca^{2+}{}_i$ oscillations. (**B** and **C**) Cyclic ADP ribose increased frequency of $Ca^{2+}{}_i$ oscillations at 10 and 50 μM. (**D**) 8-Br-cADPR prevented the effect of cADPR on $Ca^{2+}{}_i$ oscillations. (**E**) Ryanodine (30 μM) did not antagonize the cADPR effect. (**F**) IP3Rs blocker 2-APB (50 μM) blocked $Ca^{2+}{}_i$ oscillations and prevented the cADPR effect. (**G**) Mean values of $Ca^{2+}{}_i$ oscillation frequencies in the absence or presence of cADPR under conditions of the effects of 10 μM ($n = 20$), 50 μM ($n = 36$), 100 μM 8-Br-cADPR plus 50 μM cADPR ($n = 23$) and 30 μM ryanodine plus 50 μM cADPR ($n = 21$) on frequency of $Ca^{2+}{}_i$ oscillations. $*P < 0.05$ *versus* before cADPR, $\#P < 0.05$ *versus* 10 μM cADPR.

fully suppressed the $Ca^{2+}{}_i$ oscillations and antagonized the enhancement on $Ca^{2+}{}_i$ oscillation frequency by cADPR (Fig. 2F). Therefore, the inhibitory effect could be related at least in part to its action on the TRPM2 channels. Indeed, as it will be described in detail below, the TRPM2 channel is likely the target of cADPR instead of the RyRs.

The quantitative data for the effects of cADPR on $Ca^{2+}{}_i$ oscillatory frequency are summarized in Figure 2G. Cyclic APDR at 10 and 50 μM significantly increased $Ca^{2+}{}_i$ oscillation frequency by 69 ± 19% and 108 ± 25%, respectively ($P < 0.05$ *versus* before cADPR). These results suggest that the cADPR-induced increase of $Ca^{2+}{}_i$ oscillation frequency is dependent on the IP3Rs-mediated pathway, but not that mediated by the RyRs.

Nucleoside transporters are responsible for the transport of cADPR

Previous studies have demonstrated that concentrative nucleoside transporters (CNTs) and equilibrative nucleoside transporters (ENTs) are responsible for the transport of external cADPR into human haematopoietic progenitors [24] and human promyelocytic leukemia (HL)-60 cells [36]. To determine whether these nucleoside transporters are present in human MSCs, the related mRNAs were examined by RT-PCR, which showed significant expression of ENT1/ENT2 and CNT1/CNT3 in the cells (Fig. 3A). Two other components of the cADPR-pathway were also present in human MSCs, the hexameric hemichannel connexin 43 (Cx43) and the bone

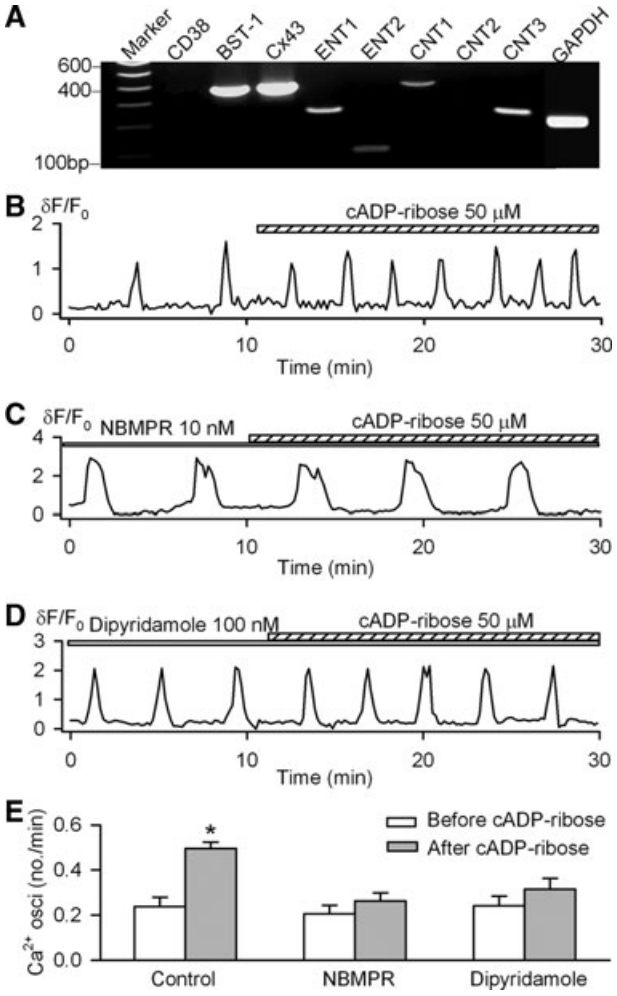

Fig. 3 Nucleoside transporters and cADPR transportation. (**A**) RT-PCR detected significant gene expression for CNT1, CNT3, ENT1, ENT2, BST-1 and Cx43. No significant CD38 gene expression was detected in human MSCs. CNT: concentrative nucleoside transporter; ENT: equilibrative nucleoside transporter; BST-1: bone marrow stroma antigen-1; Cx43: connexin 43. (**B**) Spontaneous $Ca^{2+}{}_i$ oscillations in a representative cell. (**C**) cADPR had no significant effect on $Ca^{2+}{}_i$ oscillations in the cell pre-treated with 10 nM NBMPR (nitrobenzylthioinosine). Similar results were obtained in a total of 10 cells. (**D**) The nucleoside transporter inhibitor dypyridamole (100 nM) prevented cADPR effect. (**E**) Mean values for the effects of 50 μM cADPR ($n = 36$), 10 nM NBMPR plus 50 μM cADPR ($n = 10$) and 100 nM dipyridamole plus 50 μM cADPR ($n = 11$) on the frequencies of $Ca^{2+}{}_i$ oscillations. $^*P < 0.05$ *versus* before cADPR.

marrow stromal cell antigen-1 (BST-1). Cx43 has been demonstrated to mediate the nicotinamide adenine dinucleotide (NAD^+) transport and it is known to be functionally interacting with the multifunctional ecto-enzymes, CD38 and/or BST-1 (also called CD157) in the plasma membrane, both catalyse the synthesis and hydrolysis of cADPR [37]. Indeed, BST-1 (CD157) [38, 39], but not CD38, was strongly expressed in human MSCs (Fig. 3A).

Nitrobenzylthioinosine (NBMPR) and dipyridamole were found to block the nucleoside transporters ENTs/CNTs [24, 36]. To investigate whether the nucleoside transporters are involved in the transportation of cADPR, human MSCs were pre-treated with NBMPR (10 nM) or dipyridamole (100 nM), and both were effective in blocking cADPR from stimulating the $Ca^{2+}{}_i$ oscillation frequency (Fig. 3C–E).

The dependence of the cADPR-effect on the TRPM2 channels

RyR mRNA expression was not found in human MSCs (Fig. S1). The negative result is not due to the primers we used for RyRs, because all three types of RyR mRNA were detected in human neuroblastoma cell line SH-SY5Y using the same primers (Fig. S1F), as reported previously [40].

To investigate whether TRPM2 channels participate in the cADPR-induced increase of $Ca^{2+}{}_i$ oscillation frequency, two structurally different inhibitors of the channel, econazole (10 μM) and clotrimazole (10 μM) [41], were tested in human MSCs. Both showed no significant effect on the spontaneous $Ca^{2+}{}_i$ oscillations, but both effectively prevented the increase of $Ca^{2+}{}_i$ oscillation frequency induced by cADPR (Fig. 4B and C). The quantitative results are summarized in Figure 4D. RT-PCR (Fig. 4E) showed the presence of the mRNA for the full length form of TRPM2, TRPM2-L, but not short form, TRPM2-S, which was also confirmed by Western blot analysis (Fig. 4F) for protein expression in human MSCs. These results suggest that the increased $Ca^{2+}{}_i$ oscillation frequency by cADPR is most likely mediated by the TRPM2 channels.

To further investigate the involvement of the TRPM2 channel in mediating the cADPR- regulation of the spontaneous $Ca^{2+}{}_i$ oscillations, siRNA molecules (Table S4) targeting human TRPM2 channel were transfected into MSCs using the lipofectamine 2000 reagent. The transfection efficiency was determined to be >90% at 4 hrs after transfection in cells transfected with green fluorescent control siRNA (data not shown). Both the mRNA and protein expression of TRPM2 were remarkably reduced by all three of the TRPM2 siRNA molecules, as compared to the control siRNA (Fig. 5A). TRPM2 protein levels were significantly reduced by 75% to 89% with the specific siRNAs (Fig. 5B and C).

The effect of cADPR on the spontaneous $Ca^{2+}{}_i$ oscillations was examined in human MSCs transfected with TRPM2 siRNAs. They were not significantly affected by the transfection of either the control siRNA or TRPM2 siRNAs. The percentage (81.3%, 26 out of 32 cells) of cells with $Ca^{2+}{}_i$ oscillations after transfection was close to that shown earlier without transfection (Fig. 1G). However, the cells transfected with TRPM2 siRNA molecules showed no response to cADPR (Figure 5E and F), whereas in cells transfected with control siRNA, cADPR retained the positive regulatory effect on the $Ca^{2+}{}_i$ oscillation frequency (Fig. 5D). The quantitative results are summarized in Figure 5G, which support the notion that cADPR is a modulator of the spontaneous $Ca^{2+}{}_i$ oscillations in human MSCs, and the effect is mediated by the TRPM2 channels.

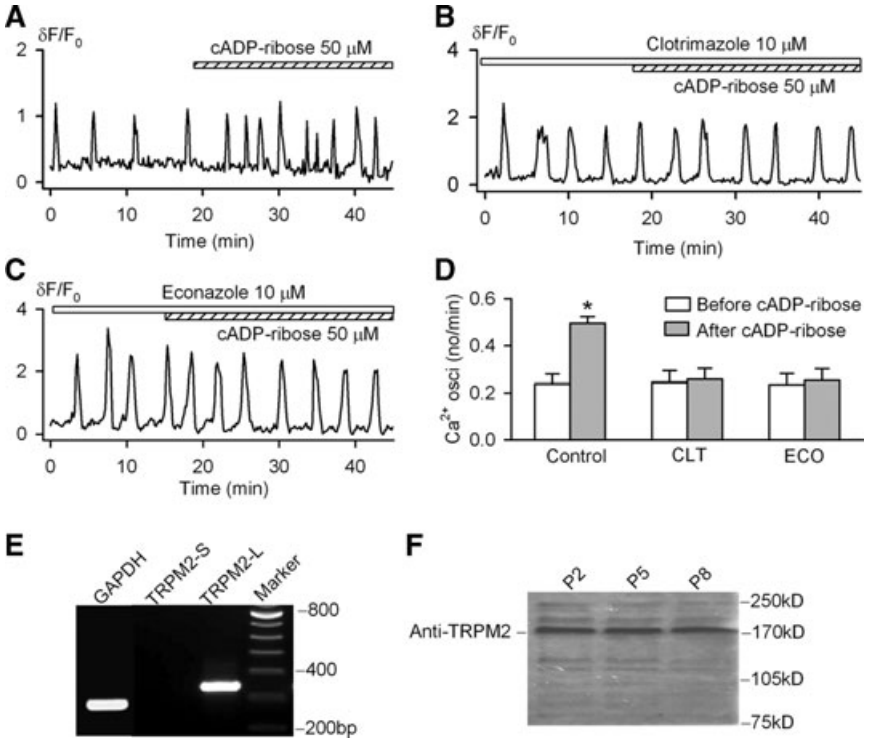

Fig. 4 TRPM2 channel and cADPR in human MSCs. (**A**) Cyclic ADP ribose increased frequency of $Ca^{2+}{}_i$ oscillations in a representative cell. (**B**) Cyclic ADP ribose had no significant effect on $Ca^{2+}{}_i$ oscillations in the cell pre-treated with the TRMP2 channel inhibitor clotrimazole. (**C**) Econazole prevented cADPR effect on $Ca^{2+}{}_i$ oscillations. (**D**) Mean values for the effects of 50 μM cADPR ($n = 36$), 10 μM clotrimazole plus 50 μM cADPR ($n = 23$) and 10 μM econazole plus 50 μM cADPR ($n = 26$) on frequency of $Ca^{2+}{}_i$ oscillations. $^*P < 0.05$ *versus* before cADPR. (**E**) RT-PCR revealed the expression of full length isoform of TRPM2 (TRPM2-L) gene. (**F**) Western blot analysis showed TRPM2 channel protein in human MSCs from passages 2, 5 and 8.

The effect of cADPR on the proliferation of human MSCs

Cell proliferation was assessed by the MTT and the ^{3}H-thymidine incorporation assays. Cyclic ADP ribose increased cell proliferation in a concentration-dependent manner and significant effects were observed at concentrations from 10 to 50 μM (Fig. 6A). At 50 μM, the cell proliferation was increased by 19 ± 7% as determined by the MTT assay. The effect was completely antagonized by co-administration of 100 μM 8-Br-cADPR (Fig. 6A). Likewise, ^{3}H-thymidine incorporation was increased by cADPR in a concentration-dependent way. At 50 μM, DNA synthesis was enhanced by 32 ± 9% and the effect was fully countered by co-application of 8-Br-cADPR as well (Fig. 6B). Consistently, the increase in the rate of DNA synthesis by cADPR was not observed in cells transfected with the TRPM2 siRNAs (Fig. 6C), whereas the effect was still seen in the cells transfected with the control siRNA ($n = 10$, $P < 0.01$). These results indicate that the enhanced cell proliferation by cADPR is mediated by the TRPM2 channel.

The intracellular mechanism of the cADPR-induced cell proliferation

To determine whether the cADPR-induced increase of proliferation is mediated by MAP kinases, we investigated the phosphorylated levels of the ERK1/2 and p38 MAP, and survival kinase Akt. Figure 7A shows that a 30-min incubation with cADPR (10 and 50 μM) increased the phosphorylation level of ERK1/2 (Thr185/Tyr187) in human MSCs, and the effect was countered by 8-Br-cADPR (Fig. 7A). The effect of cADPR on phosphorylated ERK1/2 was time dependent. The increase of ERK1/2 phosphrylation level was maximal at 60 min., and the effect remained significant at 180 min. (Fig. 7B). However, the increase of phosphorylated ERK1/2 by cADPR was remarkably reduced in the cells transfected with molecule A of TRPM2 siRNAs. Cyclic ADPR (50 μM, 60 min. incubation) only induced a slight increase of phosphorylated level of ERK1/2 in TRPM2 siRNA ($n = 3$, $P =$ NS) (Fig. 7C).

On the other hand, the phosphorylation levels of Akt (Thr308/Ser473), p38 MAPK (Thr180/Tyr182) and JNK (Thr183/Tyr185) were not significantly affected by cADPR (10 or 50 μM) in human MSCs (Fig. 7D–G). These results showed the specificity of the signalling cascade activated by cADPR in human MSCs, linking *via* ERK1/2, but not Akt, p38 MAPK or JNK. Consistently, it is well known that ERK1/2 is involved in promoting cell proliferation [42].

The lack of effect of cADPR on adipogenesis and osteogenesis in human MSCs

The effect of cADPR on adipogenesis was determined in human MSCs by application of cADPR (50 μM) in the adipogenic induction

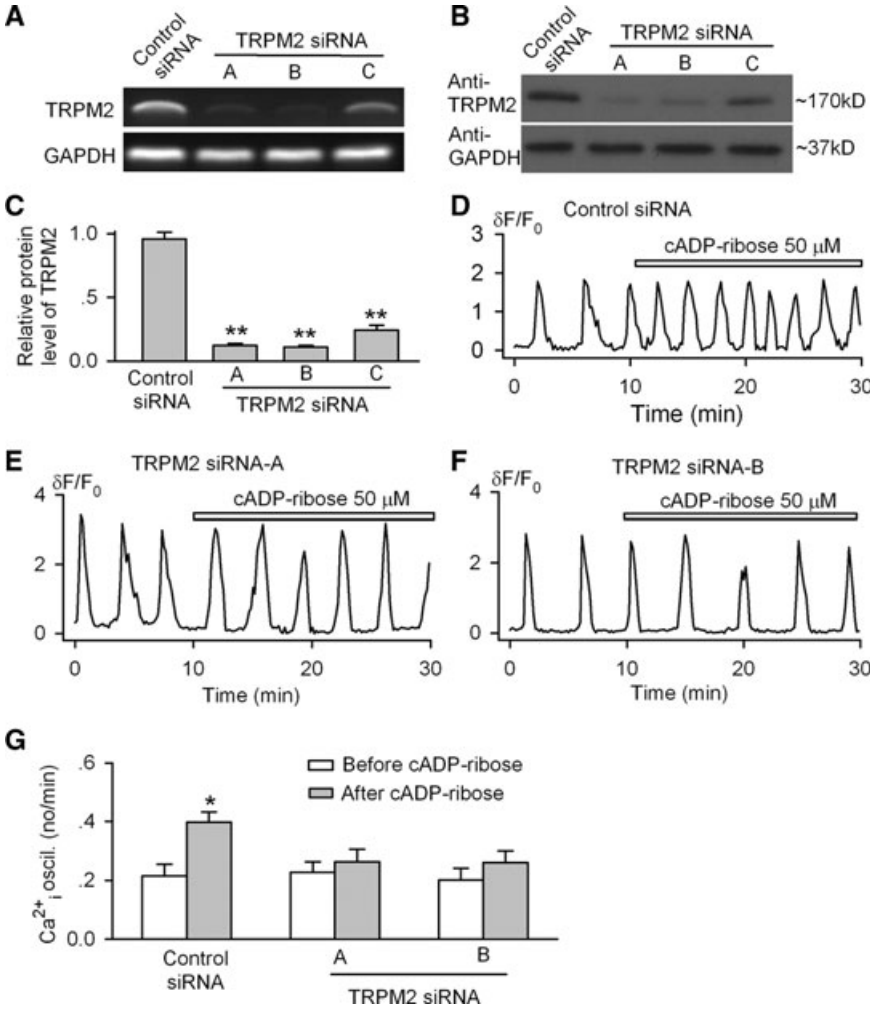

Fig. 5 Knockdown of TRPM2 channel and cADPR effect on $Ca^{2+}{}_i$ oscillations. (**A**) RT-PCR images showed the reduced gene expression of TRPM2 channel after transfection (72 hrs) with the specific siRNA A, B and C. (**B**) Western blot analysis showed decreased TRPM2 channel protein by the specific siRNA A, B and C. (**C**) The mean relative values of TRPM2 channel protein in cells transfected with control siRNA or with the specific siRNAs. $n = 3$, $^{**}P < 0.01$ *versus* control siRNA. (**D**) Cyclic ADP ribose increased the frequency of $Ca^{2+}{}_i$ oscillations in cells transfected with control siRNA. (**E** and **F**) Cyclic ADP ribose had no effect on $Ca^{2+}{}_i$ oscillations in cells transfected with TRPM2 siRNA A or B. (**G**) Mean values for the effects of 50 μM cADPR on frequency of $Ca^{2+}{}_i$ oscillations in cells transfected with TRMP2 siRNA A ($n = 26$) and B ($n = 27$), and control siRNA ($n = 25$). $^{*}P < 0.05$ *versus* before cADPR.

medium. Three cycles (3 days/cycle) of induction were employed and Oil red O staining performed at each cycle showed an increase of adipogenesis with each cycle, but cADPR had no effect on adipogenesis (Fig. S2A), and no difference of PPAR-γ expression was observed in the differentiated cells treated with and without cADPR application (Fig. S2B). The spontaneous $Ca^{2+}{}_i$ oscillations disappeared as differentiation progressed, and cADPR (50 μM) could not induce $Ca^{2+}{}_i$ changes before, during and after adipogenesis (Fig. S2C).

The effect of cADPR on osteogenesis was determined in human MSCs by application of cADPR (50 μM) in the osteogenic induction medium for 21 days, with fresh medium replacement every 3 days. Mineralization staining with Alizarin red S displayed the increased osteogenesis with prolonged induction time and cADPR again had no significant effect on osteogenesis as compared to the control group (Fig. S3A), and no difference of osteocalcin protein expression was observed in the differentiated cells treated with and without cADPR application (Fig. S3B). Similar to that observed in adipogenesis, the spontaneous $Ca^{2+}{}_i$ oscillations disappeared after osteogenesis, and cADPR (50 μM) could not induce $Ca^{2+}{}_i$ changes during osteogenesis either (Fig. S3B).

Discussion

Cyclic ADP ribose is a well-known endogenous Ca^{2+} mobilizing cyclic nucleoside that targets the $Ca^{2+}{}_i$ stores in the endoplasmic reticulum in many cell types and species covering protozoa, plants and animals, including human beings [15, 17]. It is formed by ADP-ribosyl cyclases (CD38 and/or BST-1) from NAD^+. cADPR has been established as a second messenger for Ca^{2+} signalling in an equally wide range of cell types [14, 15, 17]. Most unexpectedly, in addition to being an intracellular second messenger, cADPR has recently been proposed to function as a non-peptide

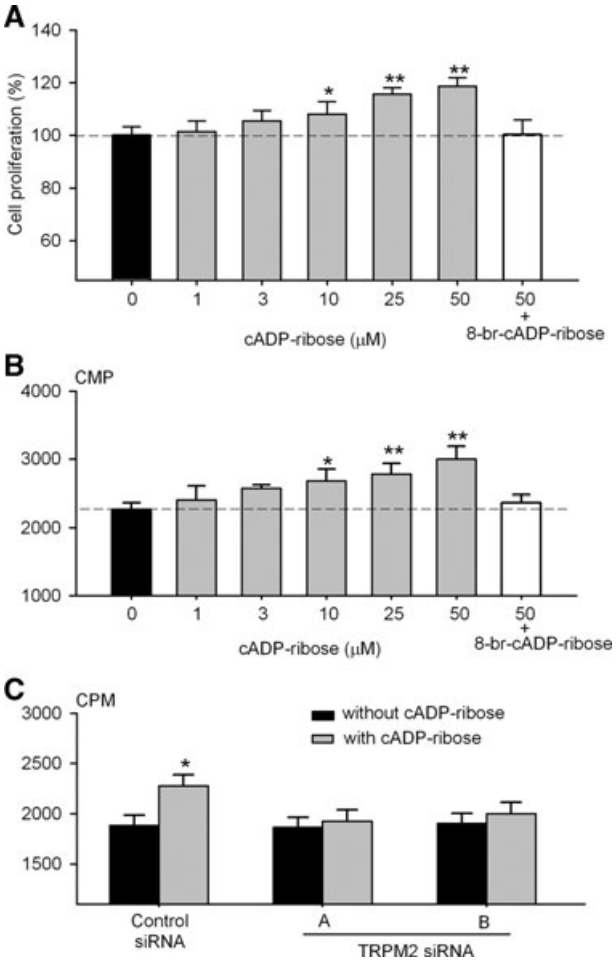

Fig. 6 Effect of cADPR on cell proliferation in human MSCs. (**A**) Cyclic ADP ribose increased cell proliferation (assessed by MTT assay) in a concentration-dependent manner. The effect was antagonized by 100 μM 8-Br-cADPR. $n = 10$, $^{*}P < 0.05$, $^{**}P < 0.01$ *versus* 0 μM cADPR. (**B**) Cyclic ADP ribose increased ^{3}H-thymidine incorporation in a concentration-dependent manner, and the effect was antagonized by 100 μM 8-Br-cADPR. $n = 10$, $^{*}P < 0.05$, $^{**}P < 0.01$ *versus* 0 μM cADPR. (**C**) Cyclic ADP ribose did not increase ^{3}H-thymidine incorporation in cells transfected with TRMP2 siRNA A or B. $n = 10$, $^{*}P < 0.05$ *versus* without cADPR application.

haematopoietic growth factor stimulating the expansion of human haematopoietic progenitors in an autocrine/paracrine fashion [21, 24, 43]. It is proposed that cells can release cytoplasmic NAD^{+} *via* the Cx43 hemichannels, and is converted extracellularly by the ecto-CD38 and/or BST-1 to cADPR. The latter is then transported back into the progenitors by the nucleoside transporters to perform its Ca^{2+} signalling function intracellularly [44]. The results presented in this study are fully consistent with this novel scheme. Hence, we show that external cADPR can increase the frequency of spontaneous $Ca^{2+}{}_{i}$ oscillations in human MSCs and stimulate their proliferation. All the components of the autocrine/paracrine pathway, Cx34, BST-1, CNTs and ENTs are well expressed in the cells (Fig. 3A) and blocking the transport function of the nucleoside transporters indeed inhibits the effects of cADPR.

The intracellular target for cADPR is generally believed to be the RyRs [14, 15, 17]. However, recent studies have demonstrated that TRPM2 channel is also a target of cADPR [18, 45, 46]. In the present study, we did not find functional or molecular evidence for the presence of the RyRs in human MSCs (Fig. S1). This is consistent with a previous report [8] and the idea that RyRs are expressed mainly in differentiated cells, but not in stem cells [47–49].

Our results strongly support the notion that the TRPM2 channel [41] is responsible for mediating the cADPR-induced increase of $Ca^{2+}{}_{i}$ oscillation frequency and cell proliferation in human MSCs. First, both the mRNA and protein of TRPM2 are strongly expressed in human MSCs. Second, blocking the TRPM2 channels pharmacologically using clotrimazole or enconazole or knocking down the channel expression specifically using siRNAs, all inhibit the effects of cADPR (Figs. 4–6). Although the effect of cADPR on IP3Rs is likely involved, the efficacy would be weaker than that on TRPM2 channels.

The TRPM2 channel was initially found to be functionally activated by ADP ribose by gating at NUDT9-H domain of the channel and acting as an intrinsic deactivation mechanism through its breakdown [50]. Further studies show that cADPR can synergize the action of ADP ribose on TRPM2 channel activation [18]. In Junket lymphocytes, cADPR can actually activate the TRPM2 channel directly and the effect is antagonized by 8-Br-cADPR, but not by the ADP-ribose antagonist, AMP. In addition, 8-Br-cADPR does not counter the activation of TRPM2 channel by ADP ribose, indicating that cADPR and ADP ribose have distinct binding sites on the TRPM2 channel [46]. In pancreatic islets, cADPR evokes Ca^{2+} entry and insulin release, and the effect is significantly diminished by the application of specific siRNAs targeting to the TRPM2 channels [45]. Consistently, we show that 8-Br-cADPR inhibits the cADPR effects in a manner similar to that exerted by either the TRPM2 antagonists or the siRNA knockdown, indicating TRPM2 is the specific target of cADPR in human MSCs.

We demonstrate in this study that the functional consequence of the increase in Ca^{2+} oscillations induced by cADPR is the stimulation of cell proliferation. Thus, blocking the enhancing effect of cADPR on Ca^{2+} oscillation using either 8-Br-cADPR or TRPM2 siRNA correspondingly inhibits the stimulation of proliferation (Fig. 6), showing the two are causally correlated. This is consistent with previous studies showing that the frequency of $Ca^{2+}{}_{i}$ sparks can determine the efficiency of gene expression in T-lymphocytes [11]. Likewise, in human MSCs the flow stress-manipulated $Ca^{2+}{}_{i}$ oscillations have been reported to regulate proliferation as well [13]. The resultant effect of the increased Ca^{2+} oscillations appears to be the simulation of the activities of signalling kinases, as shown in HeLa cells [12]. Indeed, we find that cADPR-promoted proliferation of human MSCs is mediated by enhancing phosphorylation of ERK1/2, but not Akt or P38 MAPK (Fig. 7). ERK1/2 is involved in

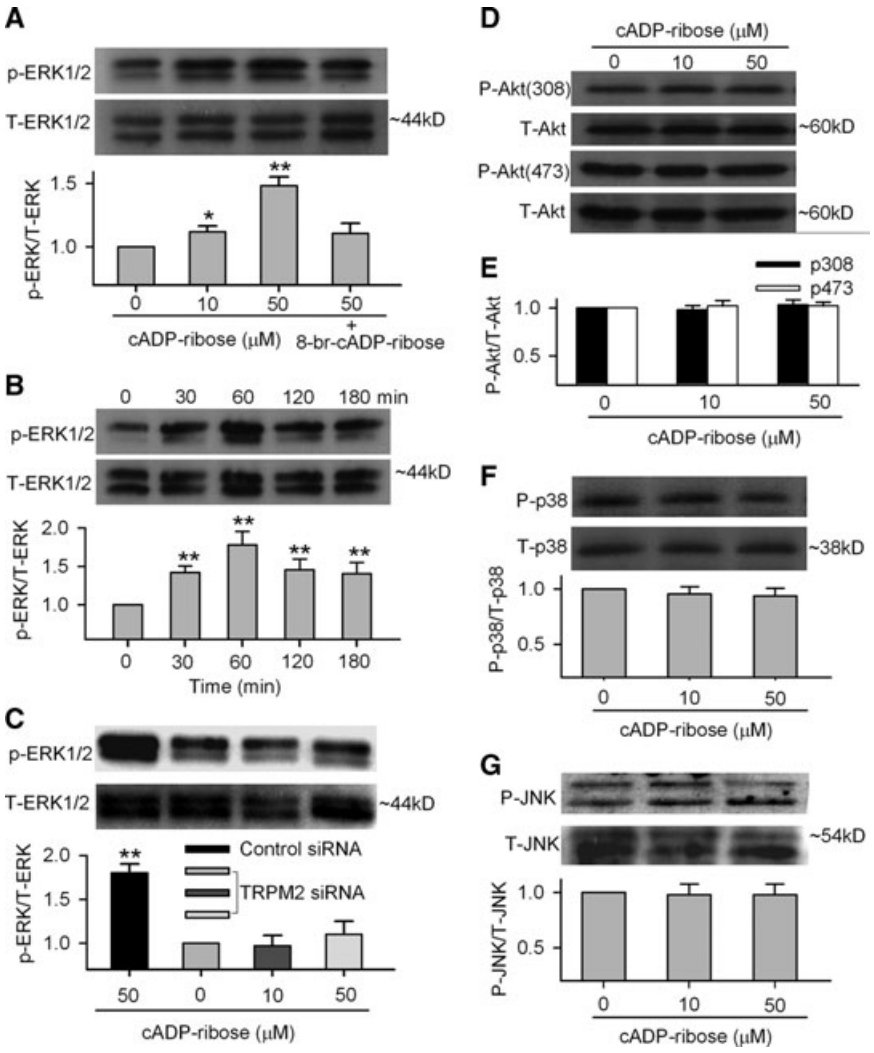

Fig. 7 Cyclic ADP ribose and proliferation-related kinases. (**A**) ERK1/2 phosphorylation at Thr185/Tyr187 was enhanced in the presence of cADPR (10 and 50 μM) for 60 min. and 8-Br-cADPR (100 μM) reduced the effect (upper panels). Mean values (lower panel) for ratio of p-ERK1/2:total ERK1/2 ($n = 3$, $^{*}P < 0.05$, $^{**}P < 0.01$ *versus* 0 μM cADPR). (**B**) Time-dependent effect of cADPR on ERK1/2 phosphorylation and mean values for ratio of p-ERK1/2:total ERK1/2 in the presence of cADPR for 30, 60, 120 and 180 min. ($n = 3$, $^{**}P < 0.01$ *versus* 0 μM cADPR). (**C**) ERK1/2 phosphorylation and mean values for ratio of p-ERK1/2:total ERK1/2 in the presence of cADPR in the cells transfected with control siRNA or TRPM2 siRNA for 72 hrs ($n = 3$, $^{**}P < 0.01$ *versus* 0 μM cADPR). (**D**) Akt1 phosphorylation at Thr308 and Ser473 was not affected by cADPR (10 and 50 μM for 60 min.). (**E**) Mean values for ratio of p-Akt(308):total Akt ($n = 3$) and p-Akt(473):total Akt ($n = 3$). (**F**) p38 MAPK phosphorylation levels at Thr180/Tyr182 were not changed when incubated with cADPR (10 and 50 μM) for 60 min. ($n = 3$). (**G**) JNK phosphorylation levels at Thr183/Tyr185 were not changed when incubated with cADPR (10 and 50 μM) for 60 min. ($n = 3$).

promoting cell proliferation [42]. This is consistent with the previous observation that the fluid flow stress-manipulated $Ca^{2+}{}_i$ oscillations increased cell proliferation is also related to increased phosphorylation of ERK1/2 in human MSCs [13].

In contrast to the positive correlation between enhancement of Ca^{2+} signalling and cell proliferation, we observe that cell differentiation, both adipogenesis and osteogenesis, leads to cessation of Ca^{2+} oscillation. Consistently, cADPR, a Ca^{2+} messenger, also shows no effect on differentiation (Figs S2 and S3). A similar dichotomic relationship between the cADPR-dependent Ca^{2+} signalling and cell proliferation *versus* differentiation is also observed in PC12 cells. Thus, activation of the cADPR-pathway is shown to simulate proliferation of PC12 cells, while blockage of the pathway accelerates their neuronal differentiation [51].

It is well known that the characteristics is not identical in human MSCs defined by surface markers and cells isolated from different sources and/or different individuals [21, 24, 52–54], and therefore an intrinsic limitation in using the isolated human MSCs should be noted. There are at least two subset populations of human MSCs (*e.g.* surface marker $CD106^{+}$ or $CD106^{-}$) demonstrated by different laboratories [21, 24, 52–54]. The expression of CD106 was found to be restricted to the $MSCA\text{-}1^{+}$ and $CD56^{-}$ MSCs subset [52]. The molecular characteristics may be different in these two subset human MSCs. For example, Scarfi and colleagues have demonstrated that the MSCs they used express surface marker CD106 in 34–78% cells and show significant differences from those (only 0.8% MSCs expressing CD106) we used in this study (Table S5). In particular, mRNAs for CD38, RyR1 and RyR3 are detected, and no spontaneous Ca^{2+} oscillations are observed in their MSCs (Scarfi *et al.*, 2008). Most importantly, however, despite these differences, both subsets MSCs are responsive to cADPR and show enhanced Ca^{2+} signalling that

leads to stimulation of cell proliferation [21], providing a strong evidence that the cADPR-pathway is of fundamental importance in regulation cell proliferation of human MSCs, independent of the population difference.

It is well recognized that human MSCs are precursors of haematopoietic stroma which plays an essential role in the bone marrow microenvironment by providing haematopoietic progenitors with soluble factors essential to their proliferation and differentiation and by preventing lymphocyte activation [1–4]. MSCs regulate haematopoiesis through the production of both growth-promoting and cytotoxic factors [55, 56] to produce biochemical signals that are produced by MSCs and active on haematopoietic stem cells, which include cADPR [21, 24, 43]. Cyclic ADPR produced by MSCs is clearly a growth promoter of human MSCs (Fig. 6) [21] and haematopoietic progenitors [24, 43].

In the present study, we limited the cell passages 2 to 5, because it has been reported that human MSCs entered senescence and lose multilineage differentiation potency during *in vitro* passaging [32–34], and biological features and gene expression profile in MSCs could vary between early passages and late passages [57]. The cells used in the present study maintained 'stem' capability, which is reflected in the differentiation experiments (Figs 1, S2 and S3).

Collectively, the present study demonstrates that application of cADPR in bath medium positively regulates the frequency of spontaneous $Ca^{2+}{}_i$ oscillations and cell proliferation in human MSCs. These effects are mediated by the nuclear transporters CNTs and/or ENTs, TRPM2 channel and the activation of the MAP kinases ERK1/2. Therefore, cADPR is a cell cycling promoter of MSCs by positive regulation of $Ca^{2+}{}_i$ oscillations. The results suggest that cADPR likely play an essential role in maintaining *in situ* normal function of bone marrow microenvironment in human beings. Whether cADPR can be used clinically for stimulating bone marrow function in patients with marrow disorders remains further studied.

Acknowledgements

This study was supported by Grants from the Research Grant Council of Hong Kong (734703M to GRL, 769107M, 768408 and 769309 to HCL, and the group grant 8CRF09 to H.F.T. and G.R.L.). Dr. R.T. was supported by a postgraduate studentship from the University of Hong Kong. We thank Dr. Darwin J. Prockop at Texas A&M Health Science Center College of Medicine Institute for Regenerative Medicine at Scott & White (through a grant from NCRR of the NIH, Grant #P40RR017447) for providing the human MSCs.

Conflict of interest

The authors confirm that there are no conflicts of interest.

Supporting Information

Additional Supporting Information may be found in the online version of this article:

Table S1 PCR primers for human adipogenic and osteogenic specific genes

Table S2 PCR primers for human genes of Ca^{2+} signals and transporters

Table S3 PCR primers for human specific genes related to cADP ribose

Table S4 siRNA sequences of TRPM2 (NM_003307)

Table S5 Flow cytometry mark results – human bone marrow MSCs

Fig. S1 Ca^{2+} signaling pathways in human MSCs. (**A**) The IP3Rs blocker 2-APB suppressed spontaneous Ca^{2+}i oscillations (n = 27). (**B**) SERCAs inhibitor CPA abolished Ca^{2+}i oscillations (n = 27). (**C**) RyRs blocker showed no significant effect on Ca^{2+}i oscillations (n = 24). (**D**) $LaCl_3$, a SOC entry blocker blocked Ca^{2+}i oscillations (n = 25). (**E**) RT-PCR results show significant mRNAs for IP3R1-3, SERCA1-3, PMCA1-3, NCX1, NCX3 and NCX4, but not for RyRs. (**F**) Messenger RNAs for RyR1-3 were detectable human SH-SY5Y neuroblastoma cells (H), but not in human MSCs (S) using three primers of RyRs in (**E**). IP3R: IP3 receptor; SERCA: sarco/endoplasmic reticulum Ca^{2+}-ATPase; PMCA: plasma membrane Ca^{2+}-ATPase. NCX: Na^{+}-Ca^{2+} exchanger; RyR: ryanodine receptor; H: total RNA extracted from human SH-SY5Y neuroblastoma cells; S: human MSCs.

Fig. S2 Effects of cADP ribose on adipogenesis in human MSCs. (**A**) Images showing adipogenic differentiation of human MSCs at induction cycle 1, 2 and 3. cADP ribose showed no significant effect on adipogenesis in human MSCs. Similar results were obtained in a total of three experiments. (**B**) No difference was found in PPAR-γ protein expression in the differentiated adipocytes (day 9) with and without the treatment of 50 μM cADPR (**C**) No spontaneous Ca^{2+}i oscillations were observed during adipogenesis on day 1, day 4 and day 9. cADP ribose did not initiate Ca^{2+}i transient or Ca^{2+}i oscillations in these cells (n = 32 for each).

Fig. S3 Effects of cADP ribose on osteogenesis in human MSCs. (**A**) Images showing the osteogenesis on day 10, day 15 and day 20 by Alizarin red S staining. cADP ribose had no significant effect on osteogenesis in human MSCs. Similar results were obtained in a total of three experiments. (**B**) No difference was found in osteocalcin protein expression in the differentiated osteocytes (day 18) with and without the treatment of 50 μM

cADPR (**C**) No spontaneous $Ca^{2+}{}_i$ oscillations were observed during osteogenesis on day 1, day 9 and day 18. Cyclic ADP ribose did not initiate $Ca^{2+}{}_i$ transient or $Ca^{2+}{}_i$ oscillations in these cells (n = 32 for each).

References

1. **Zou Z, Zhang Y, Hao L, *et al.*** More insight into mesenchymal stem cells and their effects inside the body. *Expert Opin Biol Ther*. 2010; 10: 215–30.
2. **Pittenger MF, Mackay AM, Beck SC, *et al*.** Multilineage potential of adult human mesenchymal stem cells. *Science*. 1999; 284: 143–7.
3. **Ball SG, Shuttleworth CA, Kielty CM.** Platelet-derived growth factor receptors regulate mesenchymal stem cell fate: implications for neovascularization. *Expert Opin Biol Ther*. 2010; 10: 57–71.
4. **Aggarwal S, Pittenger MF.** Human mesenchymal stem cells modulate allogeneic immune cell responses. *Blood*. 2005; 105: 1815–22.
5. **Smits AM, van Vliet P, Hassink RJ, *et al.*** The role of stem cells in cardiac regeneration. *J Cell Mol Med*. 2005; 9: 25–36.
6. **Liang X, Su YP, Kong PY, *et al.*** Human bone marrow mesenchymal stem cells expressing SDF-1 promote hematopoietic stem cell function of human mobilised peripheral blood CD34(+) cells *in vivo* and *in vitro*. *Int J Radiat Biol*. 2010; 86: 230–7.
7. **Berridge MJ, Lipp P, Bootman MD.** The versatility and universality of calcium signalling. *Nat Rev Mol Cell Biol*. 2000; 1: 11–21.
8. **Kawano S, Shoji S, Ichinose S, *et al.*** Characterization of Ca(2+) signaling pathways in human mesenchymal stem cells. *Cell Calcium*. 2002; 32: 165–74.
9. **Kawano S, Otsu K, Shoji S, *et al.*** Ca(2+) oscillations regulated by Na(+)-Ca(2+) exchanger and plasma membrane Ca(2+) pump induce fluctuations of membrane currents and potentials in human mesenchymal stem cells. *Cell Calcium*. 2003; 34: 145–56.
10. **Kawano S, Otsu K, Kuruma A, *et al.*** ATP autocrine/paracrine signaling induces calcium oscillations and NFAT activation in human mesenchymal stem cells. *Cell Calcium*. 2006; 39: 313–24.
11. **Dolmetsch RE, Xu K, Lewis RS**. Calcium oscillations increase the efficiency and specificity of gene expression. *Nature*. 1998; 392: 933–6.
12. **Kupzig S, Walker SA, Cullen PJ.** The frequencies of calcium oscillations are optimized for efficient calcium-mediated activation of Ras and the ERK/MAPK cascade. *Proc Natl Acad Sci USA*. 2005; 102: 7577–82.
13. **Riddle RC, Taylor AF, Genetos DC, *et al.*** MAP kinase and calcium signaling mediate fluid flow-induced human mesenchymal stem cell proliferation. *Am J Physiol Cell Physiol*. 2006; 290: C776–84.
14. **Lee HC.** Multiplicity of Ca^{2+} messengers and Ca^{2+} stores: a perspective from cyclic ADP-ribose and NAADP. *Curr Mol Med*. 2004; 4: 227–37.
15. **Lee HC.** Physiological functions of cyclic ADP-ribose and NAADP as calcium messengers. *Annu Rev Pharmacol Toxicol*. 2001; 41: 317–45.
16. **Guse AH.** Regulation of calcium signaling by the second messenger cyclic adenosine diphosphoribose (cADPR). *Curr Mol Med*. 2004; 4: 239–48.
17. **Guse AH.** Biochemistry, biology, and pharmacology of cyclic adenosine diphosphoribose (cADPR). *Curr Med Chem*. 2004; 11: 847–55.
18. **Kolisek M, Beck A, Fleig A, *et al.*** Cyclic ADP-ribose and hydrogen peroxide synergize with ADP-ribose in the activation of TRPM2 channels. *Mol Cell*. 2005; 18: 61–9.
19. **Okamoto H.** The CD38-cyclic ADP-ribose signaling system in insulin secretion. *Mol Cell Biochem*. 1999; 193: 115–8.
20. **Podesta M, Zocchi E, Pitto A, *et al.*** Extracellular cyclic ADP-ribose increases intracellular free calcium concentration and stimulates proliferation of human hemopoietic progenitors. *FASEB J*. 2000; 14: 680–90.
21. **Scarfi S, Ferraris C, Fruscione F, *et al.*** Cyclic ADP-ribose-mediated expansion and stimulation of human mesenchymal stem cells by the plant hormone abscisic acid. *Stem Cells*. 2008; 26: 2855–64.
22. **Zocchi E, Podesta M, *et al.*** Paracrinally stimulated expansion of early human hemopoietic progenitors by stroma-generated cyclic ADP-ribose. *FASEB J*. 2001; 15: 1610–2.
23. **Podesta M, Pitto A, Figari O, *et al.*** Cyclic ADP-ribose generation by CD38 improves human hemopoietic stem cell engraftment into NOD/SCID mice. *FASEB J*. 2003; 17: 310–2.
24. **Podesta M, Benvenuto F, Pitto A, *et al.*** Concentrative uptake of cyclic ADP-ribose generated by BST-1^+ stroma stimulates proliferation of human hematopoietic progenitors. *J Biol Chem*. 2005; 280: 5343–9.
25. **Li GR, Sun H, Deng X, *et al.*** Characterization of ionic currents in human mesenchymal stem cells from bone marrow. *Stem Cells*. 2005; 23: 371–82.
26. **Deng XL, Sun HY, Lau CP, *et al.*** Properties of ion channels in rabbit mesenchymal stem cells from bone marrow. *Biochem Biophys Res Commun*. 2006; 348: 301–9.
27. **Tao R, Lau CP, Tse HF, *et al.*** Regulation of cell proliferation by intermediate-conductance Ca^{2+}-activated potassium and volume-sensitive chloride channels in mouse mesenchymal stem cells. *Am J Physiol Cell Physiol*. 2008; 295: C1409–16.
28. **Tao R, Lau CP, Tse HF, *et al.*** Functional ion channels in mouse bone marrow mesenchymal stem cells. *Am J Physiol Cell Physiol*. 2007; 293: C1561–7.
29. **Hu R, He ML, Hu H, *et al.*** Characterization of calcium signaling pathways in human preadipocytes. *J Cell Physiol*. 2009; 220: 765–70.
30. **Chen JB, Tao R, Sun HY, *et al.*** Multiple Ca^{2+} signaling pathways regulate intracellular Ca^{2+} activity in human cardiac fibroblasts. *J Cell Physiol*. 2010; 223: 68–75.
31. **Krampera M, Pasini A, Rigo A, *et al.*** HB-EGF/HER-1 signaling in bone marrow mesenchymal stem cells: inducing cell expansion and reversibly preventing multilineage differentiation. *Blood*. 2005; 106: 59–66.
32. **Fehrer C, Lepperdinger G.** Mesenchymal stem cell aging. *Exp Gerontol*. 2005; 40: 926–30.
33. **Sethe S, Scutt A, Stolzing A.** Aging of mesenchymal stem cells. *Ageing Res Rev*. 2006; 5: 91–116.

34. **Baxter MA, Wynn RF, Jowitt SN, *et al.*** Study of telomere length reveals rapid aging of human marrow stromal cells following *in vitro* expansion. *Stem Cells*. 2004; 22: 675–82.
35. **Togashi K, Inada H, Tominaga M.** Inhibition of the transient receptor potential cation channel TRPM2 by 2-aminoethoxydiphenyl borate (2-APB). *Br J Pharmacol*. 2008; 153: 1324–30.
36. **Guida L, Franco L, Bruzzone S, *et al.*** Concentrative influx of functionally active cyclic ADP-ribose in dimethyl sulfoxide-differentiated HL-60 cells. *J Biol Chem*. 2004; 279: 22066–75.
37. **Malavasi F, Deaglio S, Funaro A, *et al.*** Evolution and function of the ADP ribosyl cyclase/CD38 gene family in physiology and pathology. *Physiol Rev*. 2008; 88: 841–86.
38. **Okuyama Y, Ishihara K, Kimura N, *et al.*** Human BST-1 expressed on myeloid cells functions as a receptor molecule. *Biochem Biophys Res Commun*. 1996; 228: 838–45.
39. **Sato A, Yamamoto S, Ishihara K, *et al.*** Novel peptide inhibitor of ecto-ADP-ribosyl cyclase of bone marrow stromal cell antigen-1 (BST-1/CD157). Biochem J. 1999; 337: 491–6.
40. **Laporte R, Hui A, Laher I**. Pharmacological modulation of sarcoplasmic reticulum function in smooth muscle. *Pharmacol Rev*. 2004; 56: 439–513.
41. **Hill K, McNulty S, Randall AD.** Inhibition of TRPM2 channels by the antifungal agents clotrimazole and econazole. *Naunyn Schmiedebergs Arch Pharmacol*. 2004; 370: 227–37.
42. **Mebratu Y, Tesfaigzi Y.** How ERK1/2 activation controls cell proliferation and cell death: is subcellular localization the answer? *Cell Cycle*. 2009; 8: 1168–75.
43. **Scarfi S, Fresia C, Ferraris C, *et al.*** The plant hormone abscisic acid stimulates the proliferation of human hemopoietic progenitors through the second messenger cyclic ADP-ribose. *Stem Cells*. 2009; 27: 2469–77.
44. **De Flora A, Zocchi E, Guida L, *et al.*** Autocrine and paracrine calcium signaling by the CD38/NAD^+/cyclic ADP-ribose system. *Ann NY Acad Sci*. 2004; 1028: 176–91.
45. **Togashi K, Hara Y, Tominaga T, *et al.*** TRPM2 activation by cyclic ADP-ribose at body temperature is involved in insulin secretion. *EMBO J*. 2006; 25: 1804–15.
46. **Beck A, Kolisek M, Bagley LA, *et al.*** Nicotinic acid adenine dinucleotide phosphate and cyclic ADP-ribose regulate TRPM2 channels in T lymphocytes. *FASEB J*. 2006; 20: 962–4.
47. **Resende RR, da Costa JL, Kihara AH, *et al.*** Intracellular Ca(2+) regulation during neuronal differentiation of murine embryonal carcinoma and mesenchymal stem cells. *Stem Cells Dev*. 2010; 19: 379–94.
48. **Fu JD, Li J, Tweedie D, *et al.*** Crucial role of the sarcoplasmic reticulum in the developmental regulation of Ca^{2+} transients and contraction in cardiomyocytes derived from embryonic stem cells. *FASEB J*. 2006; 20: 181–3.
49. **Li X, Yu X, Lin Q, *et al.*** Bone marrow mesenchymal stem cells differentiate into functional cardiac phenotypes by cardiac microenvironment. *J Mol Cell Cardiol*. 2007; 42: 295–303.
50. **Perraud AL, Fleig A, Dunn CA, *et al.*** ADP-ribose gating of the calcium-permeable LTRPC2 channel revealed by Nudix motif homology. *Nature*. 2001; 411: 595–9.
51. **Yue J, Wei W, Lam CM, *et al.*** CD38/cADPR/Ca^{2+} pathway promotes cell proliferation and delays nerve growth factor-induced differentiation in PC12 cells. *J Biol Chem*. 2009; 284: 29335–42.
52. **Battula VL, Treml S, Bareiss PM, *et al.*** Isolation of functionally distinct mesenchymal stem cell subsets using antibodies against CD56, CD271, and mesenchymal stem cell antigen-1. *Haematologica*. 2009; 94: 173–84.
53. **Barbero A, Grogan SP, Mainil-Varlet P, *et al.*** Expansion on specific substrates regulates the phenotype and differentiation capacity of human articular chondrocytes. *J Cell Biochem*. 2006; 98: 1140–9.
54. **Lee HJ, Choi BH, Min BH, *et al.*** Changes in surface markers of human mesenchymal stem cells during the chondrogenic differentiation and dedifferentiation processes *in vitro*. *Arthritis Rheum*. 2009; 60: 2325–32.
55. **Dazzi F, Ramasamy R, Glennie S, *et al.*** The role of mesenchymal stem cells in haemopoiesis. *Blood Rev*. 2006; 20: 161–71.
56. **Phinney DG.** Biochemical heterogeneity of mesenchymal stem cell populations: clues to their therapeutic efficacy. *Cell Cycle*. 2007; 6: 2884–9.
57. **Vacanti V, Kong E, Suzuki G, *et al.*** Phenotypic changes of adult porcine mesenchymal stem cells induced by prolonged passaging in culture. *J Cell Physiol*. 2005; 205: 194–201.